Inhibition Due to the Interaction of Polyethylene Glycol, Chloride, and Copper in Plating Baths: A Surface-Enhanced Raman Study

Z. Vivian Feng, Xiao Li, and Andrew A. Gewirth*

Department of Chemistry and Fredrick Seitz Materials Research Laboratory, University of Illinois at Urbana-Champaign, Urbana, Illinois 61801

Received: April 3, 2003; In Final Form: May 27, 2003

The synergic effect of poly(ethylene glycol) together with chloride ion for inhibiting copper deposition in copper electroplating has been of particular interest for some time. In this study, the potential-dependent behavior of poly(ethylene glycol), with or without chloride ion in a copper electroplating bath is investigated using the surface-enhanced Raman spectroscopy technique. The presence of chloride proves to play a significant role in enhancing PEG adsorption to the Cu electrode surface. More importantly, spectroscopic evidence strongly suggests the formation of a PEG−Cu−Cl complex. By comparing experiment with vibrational modes calculated by using the Hartree−Fock method with a 3-21G* basis set, the structure of this complex is proposed to be a three-coordinated Cu center with two oxygen atoms from PEG and one chloride ligand.

1. Introduction

Electrolytic deposition of Cu is seeing renewed attention because of its importance in interconnect fabrication in microelectronic devices.[1] Small amounts of organic and inorganic reagents are employed in commercial electroplating baths as additives in order to obtain desirable deposit morphology and texture.[2,3] Some of these additives act as "accelerators" which work to decrease the overpotential for deposition relative to additive free solutions. Conversely, other additives act as "inhibitors", which increase the overpotential relative to the additive-free case. Combinations of additives are typically used to impart desirable characteristics such as high throwing power,[4] superconformal deposition,[1] and the like.

Poly(ethylene glycol) (PEG) is an additive used commonly to achieve high throwing-power and is also used in baths which produce superconformal deposition.[5] However, these traits require the presence of Cl^- as another constituent of the plating bath. By itself, PEG adsorbs only weakly on bare Cu surfaces. However, in the presence of Cl^-, PEG forms a physical diffusion barrier that suppresses electrodeposition at a given potential or, alternatively, increases the potential required to maintain a given current.[6,7]

Because of the importance of the PEG−Cl^- inhibitor, many research groups have addressed the synergic effect of PEG with chloride.[5,8−12] Since PEG by itself acts as a weak inhibitor, Cl^- is thought to facilitate the polymer adsorption process. By examining the degree of inhibition as a function of the degree of polymerization of the PEG, Yokoi et al.[8] proposed that PEG forms a pseudocrown moiety with Cu^+ or Cu^{2+} coordinated through the oxygen backbone of the polymer. They proposed that this complex would be more tightly adsorbed to the Cu surface via an electrostatic interaction when negatively charged Cl^- is present on the surface. On the basis of the behavior of an analogous complex,[13] Stoychev et al.[10] proposed that PEG adopted a complex structure involving Cu^{2+}, chloride, PEG, and water molecules. However, a detailed molecular-based understanding of the synergy between these constituents is lacking.

One way in which detailed molecular understanding can be produced is via vibrational spectroscopy. Surface-enhanced Raman spectroscopy (SERS) measurements which yield considerable insight into the nature of molecular species at the Cu/electrolyte interface are almost tailor-made for the Cu deposition problem. SERS is easily obtained from the as-deposited Cu surface, and can be obtained under potential control with sufficient electrolyte above the interface to obviate the thin layer effects which can plague infrared reflection adsorption measurements.[14−16] SERS is also known for its high sensitivity for less concentrated solution species, which is ideal for studies on such additive systems. Since the vibrational modes for metal halide and metal oxygen bands are known to exist at relatively low frequencies, SERS is highly advantageous for studying such vibrations.

There have been two studies of the PEG−Cl^- system using SERS.[7,9] Hope et al. showed that the presence of Cl^- is essential for PEG adsorption on Cu surfaces.[9] Healy et al. proposed that PEG can be adsorbed in two different forms. The first of these is a complex with copper−chloride near the Cu open circuit potential, while the other is neutral PEG molecule at the more negative potentials where copper plating actually occurs. Unfortunately, neither study provided a detailed spectral analysis nor peak assignment, and this makes molecular-based understanding problematic.

In this paper, we utilize detailed, systematic SERS measurements to examine the complex formed on a Cu surface in an acidic solution containing PEG and Cl^-. The spectroscopy reveals the essential features of this complex and with help of calculations we propose a structure.

2. Experimental Section

All solutions were prepared with ultrapure water (Milli-Q UV plus, Millipore Inc., 18.2 MΩ cm). Reagent grade H_2SO_4 (Baker, UltrexII), $CuSO_4 \cdot 5H_2O$ (99.99% Aldrich), KCl (99.6%, Fisher), KBr (99%, MCB reagents), and poly(ethylene glycol)

* Author to whom correspondence should be addressed. Tel: 217-333-8329. Fax: 217-333-2685. E-mail: agewirth@uiuc.edu.

10.1021/jp034875m CCC: $25.00
Published on Web 07/24/2003

($H(OCH_2CH_2)_nOH$, MW = 3400, $d = 1.204$, Aldrich) were used for preparing solutions. The blank electrolyte solution contained 10 mM $CuSO_4$ and 0.1 M H_2SO_4. Three different additive-containing solutions were examined, containing: 300 ppm PEG (equivalent to 88 μM), 2 mM KCl, and 2 mM KCl + 300 ppm PEG.

The polycrystalline Cu (Monocrystals Inc.) substrate was prepared in the following way to enhance its SERS activity: following mechanical and electrochemical polishing, the copper electrode was electrochemically roughened by 15 oxidation−reduction cycles in 0.1 M KCl solution. The potential was swept at 100 mV/s between −0.96 and 0.44 V vs Ag/AgCl. It was then held at −0.96 V vs Ag/AgCl for 10 s after each cycle in order to desorb any halide. To electrochemically roughen the polycrystalline Au sample (Monocrystals Inc.), the potential was first held at −1.36 V vs Ag/AgCl for 10 min and then −0.26 V for 2 min. The potential was then swept at 750 mV/s from −0.26 to 1.24 V vs Ag/AgCl and back for 20 oxidation−reduction cycles. The potential was then held at −0.56 V for 2 min. After roughening, both crystals were rinsed with a copious amount of ultrapure water.

The electrochemical cell design and the laser system have been described elsewhere.[17] The spectral resolution was estimated to be 3 to 5 cm^{-1}. The spectral acquisition time was typically 30 or 60 s, depending on the intensity of the Raman response. Potential was applied between −0.60 and 0.10 V vs Ag/AgCl with a 0.10 V increment. The system was allowed to equilibrate for two minutes at each potential before acquiring spectra. All potentials reported here are with respect to the Ag/AgCl electrode. The spectra from Cu surfaces reported here are as obtained without any baseline correction.

Calculations were undertaken utilizing the Spartan program. This calculational package provides optimized geometries constructed by using the ab initio Hartree−Fock method and a 3-21G* basis set. Once the energy of the model was minimized, the frequencies and the vibrational modes of the model compounds were calculated using the same method and basis set. The calculated frequencies were multiplied by 0.90 to account for electronic correlation effects.[17]

3. Results

3.1. Raman Spectroscopy. To identify the peaks from the SERS spectra, normal Raman spectra of PEG powder and of solutions with various additives were obtained.

3.1.1. PEG Powder. Figure 1a shows the normal Raman spectrum obtained from a pressed pellet of PEG powder. In these spectra, bands are observed at 277, 361, 534, 580, 845, 857, and 932 cm^{-1}, in agreement with that reported by Matsuura et al.[18,19] Detailed assignments for these bands are given in Table 1. The 857 and 845 cm^{-1} bands are associated with C−O−C stretches and CH_2 rocking modes, which are known to be conformation-sensitive.[18−23] The lower frequency region, from 200 to 600 cm^{-1} is mainly populated with deformation of the C−O−C skeletal bonds. Previous work has emphasized that the structure of PEG in dilute aqueous solution is similar to the helix found in the solid state, assuming the trans−gauche−trans (tgt) conformation around the successive O−C−C−O bonds.[18,24,25]

3.1.2. Solution Spectra. The normal Raman spectra of three electrolytic solutions containing $CuSO_4 + H_2SO_4$, $CuSO_4 + H_2SO_4 + Cl^-$, and $CuSO_4 + H_2SO_4 + Cl^- +$ PEG are presented in Figure 1b. The major component of all three solutions is H_2SO_4, and most of the bands in Figure 1b are associated with vibrations of SO_4^{2-} and HSO_4^-.[26−28] A detailed peak assignment is given in Table 2. When PEG is added to the solution, two additional peaks are observed at 850 and 809 cm^{-1}. The first is the C−O−C stretch of PEG seen in the solid spectrum in Figure 1a, while the second is associated with a CH_2 rock or CH_2 twist.[19] The feature at around 800 cm^{-1} is observed only in liquid or aqueous states of PEG, but not in the solid PEG spectrum.[25]

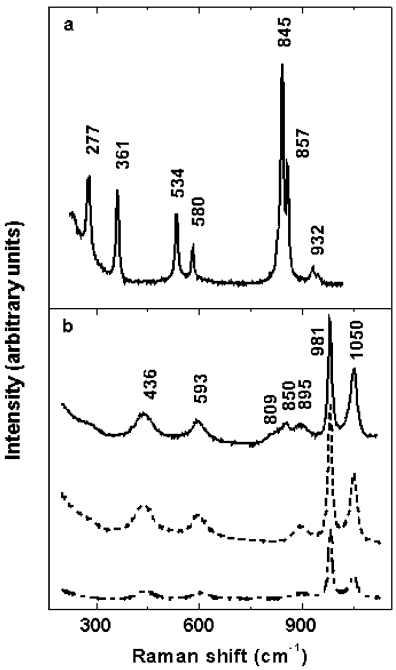

Figure 1. Normal Raman spectra of (a) pressed poly(ethylene glycol) powder and (b) 10 mM $CuSO_4$ + 0.1 M H_2SO_4 (dotted dashed line), 2 mM KCl + 10 mM $CuSO_4$ + 0.1 M H_2SO_4 (short dashed line), and 88 μM poly(ethylene glycol) + 2 mM KCl + 10 mM $CuSO_4$ + 0.1 M H_2SO_4 (solid line).

TABLE 1: Normal Raman Band Assignments for Pressed Polyethylene Glycol Powder

present study	reference 23		references 18 and 19	
277	274	δ OCC	282	
361	360	δ COC	366	skeletal
534	531	δ OCC	537	deformation
580			584	
845	845	r CH_2	845	ν CO, r CH_2
857	860	ν CO	862	ν CO, r CH_2
932			934	ν CO, r CH_2

3.2. SERS. *3.2.1. Cu Electrode Surface*. To study the Cu surface, SERS spectra in blank electrolyte ($CuSO_4 + H_2SO_4$), with chloride, with PEG, and with both chloride and PEG were taken.

3.2.1.1. No Additive. Figure 2 shows the spectra of a polycrystalline Cu surface in a solution containing 10 mM $CuSO_4$ and 0.1 M H_2SO_4 at various potentials while scanning anoidically (left) and cathodically (right). A dominant peak appears at 970 cm^{-1}, labeled as peak A. This peak is associated with the S−O symmetric stretch of sulfate, and has been reported in other SERS studies of Cu surfaces in sulfate-containing solutions.[26,27,29,30] This strong peak shows that the surface is predominately covered by the adsorbed sulfate anions from blank electrolyte. The peak is red-shifted by ca. 10 cm^{-1} relative to the solution band, a feature that has been associated with removal of electron density from the S−O bond due to chemisorption on the Cu surface. The potential dependence of peak A mimics that reported earlier.[27] The diminution of SER intensity at positive potentials is possibly associated with (a) changes in surface conditions giving rise to SER enhancement,

TABLE 2: Normal Raman and SERS Band Assignments for Solutions Containing PEG, KCl, $CuSO_4$, and H_2SO_4

peak position		literature	calculated		
normal Raman	SERS	value	value	assignment	refs
	260−270 (H)	-	265∼267	υ Cu−Cl (in complex)	-
	289−302 (D)	290−295	-	υ Cu−Cl	29, 30, 37
436	414 (F)	438	-	υ HSO_4^-	26−28
	465 (K)	460	460	υ_{sym} Cu−O (in complex)	31
	510 (L)	525	504	υ_{as} Cu−O (in complex)	40
593	-	593	-	υ HSO_4^-	26−28
	599−620 (C)	600−625	-	δ (bend) SO_4^{2-}	27, 31
	670 (I)	-	696	δ O−C−C−O (in complex)	
	715 (G)				
	790 (E)				
850	852−858 (J)	850	847	υ C−O−C	18−23
895	-	896	-	υ S−O(H) (HSO_4^-)	26−28
981	963−978 (A)	982 (Raman) 971 (SERS)	-	υ sym. SO_4^{2-}	26, 27, 29, 30
1050	1027−1037 (B)	1051	-	υ sym. HSO_4^-	26, 29, 30

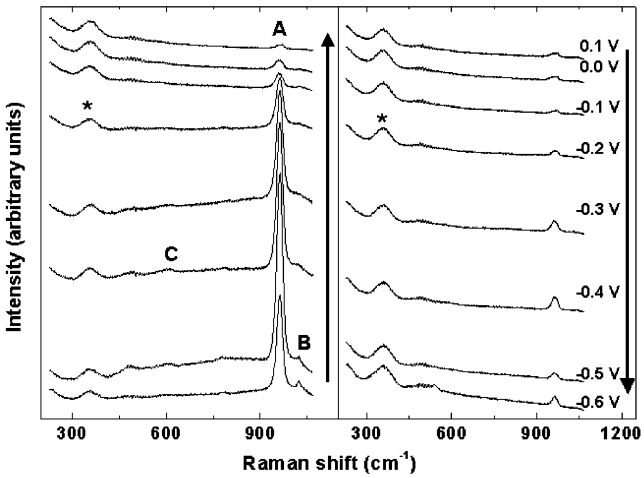

Figure 2. Surface Enhanced Raman spectra (250−1100 cm^{-1} region) of Cu(poly) in 10 mM $CuSO_4$ + 0.1 M H_2SO_4 at various potentials during anodic steps (left panel) and cathodic steps (right panel).

(b) replacement by a surface water or oxide species, or (c) changes in sulfate packing on the Cu surface.

Figure 2 also reveals a weak band at 1030 cm^{-1} (peak B) observed at potentials negative of −0.5 V. By reference to the band at 1050 cm^{-1} in the solution spectra, peak B is assigned to the symmetric S−O stretch of the bisulfate anion. The potential dependence and the 20 cm^{-1} red-shift of this band relative to that in the solution spectrum suggest that the bisulfate ion is chemisorbed on Cu surfaces. In a control experiment examining the Cu surface immersed in a solution containing 0.1 M H_2SO_4 without added $CuSO_4$, this band is not observed in the SERS (spectra not shown). Niaura et al. also did not observe the 1030 cm^{-1} band in a solution without added $CuSO_4$.[27] However, Brown et al. did observe this band—with no potential dependence—in a solution containing 2 M H_2SO_4.[26,29,30] The presence of peak B in solution containing Cu^{2+} suggests that Cu^{2+} may have an enhancement to the chemisorption of the bisulfate species.

A weak and broad band (peak C) can be observed between 600 and 620 cm^{-1}, and is assigned to the stretch of a Cu_2O species.[27,31] We also observed in an in situ AFM study that ordered oxygen (or oxygen-like) chains grow on Cu single-crystal surfaces in acidic media.[32,33] The broad band at 370−390 cm^{-1} is likely associated with a laser line from the dye laser used in these measurements.

Spectra obtained following addition of 88 μM PEG to the 0.1 M H_2SO_4 + 10 mM $CuSO_4$ solution used above led to spectra virtually identical to those reported in Figure 2. There are no additional features in the spectrum that could be associated with PEG. This suggests that PEG by itself is not strongly adsorbed to the Cu surface, a conclusion also obtained in several other electrochemical and ellipsometry studies.[2,5,34−36]

3.2.1.2. With Cl^-. Figure 3 shows potential dependent SERS obtained from a solution containing 2 mM Cl^- in addition to the 0.1 M H_2SO_4 + 10 mM $CuSO_4$ used previously. The spectra show some dramatic changes relative to Figure 2. A significant peak (peak D) with a maximum that ranges from 289 cm^{-1} at −0.6 V to 302 cm^{-1} at 0.1 V is observed in the spectrum. The peak is attributed to the Cu−Cl stretch,[29,30,37] and is a clear indication that chloride is adsorbed on the Cu surface. The peak intensity increases as the potential moves to more positive values, which is the behavior expected for an anion adsorbed on the Cu surface.

Interestingly, peak A (sulfate, S−O stretch) is not observed in these spectra, while peak B (bisulfate S−O stretch) remains with a potential dependence now that is expected for an anion on a metal. The disappearance of peak A was also noted in a previous study in chloride-containing solutions.[27] The presence of peak B indicates that bisulfate is coadsorbed with the Cl^- on Cu, but sulfate is not. A possible explanation for this behavior may relate to the decreased charge presented by bisulfate relative to sulfate. It is possible that the adsorbed Cl^- on the Cu surface may repel the doubly charged SO_4^{2-}. However, HSO_4^- with one negative charge may still remain on the surface with Cl^-. Peak C which is associated with the stretching of Cu_2O in Figure 2 disappears in these spectra as well. The elimination of this peak upon addition of chloride ion agrees with what Chan et al. have observed.[31]

There are three weaker features at 790 cm^{-1} (peak E), 414 cm^{-1}(peak F), and 715 cm^{-1} (peak G) also observed in the spectra shown in Figure 3. The energy of peak F, is close to the 436 cm^{-1} peak seen in the solution spectrum presented in Figure 1b. This peak is assigned to one of the stretching modes of HSO_4^- species in solution. Peak F is likely associated with this same molecule adsorbed or near the Cu electrode surface.

The origins of peaks E and G are not obvious. The inset to Figure 3 shows a plot of the peak intensities of peaks E and G, compared with that for peak B, which is associated with bisulfate. The identical potential dependence of these bands suggests that all three peaks are related to the same species.

To clarify the identity of peaks E and G, we obtained SERS from the Cu surface immersed in a solution where KCl was replaced with KBr (spectra not shown). These spectra featured all of peaks B, E, F, and G at essentially the same energies. Thus, none of these peaks can be associated with the halide, a conclusion already advanced for peaks B and F.

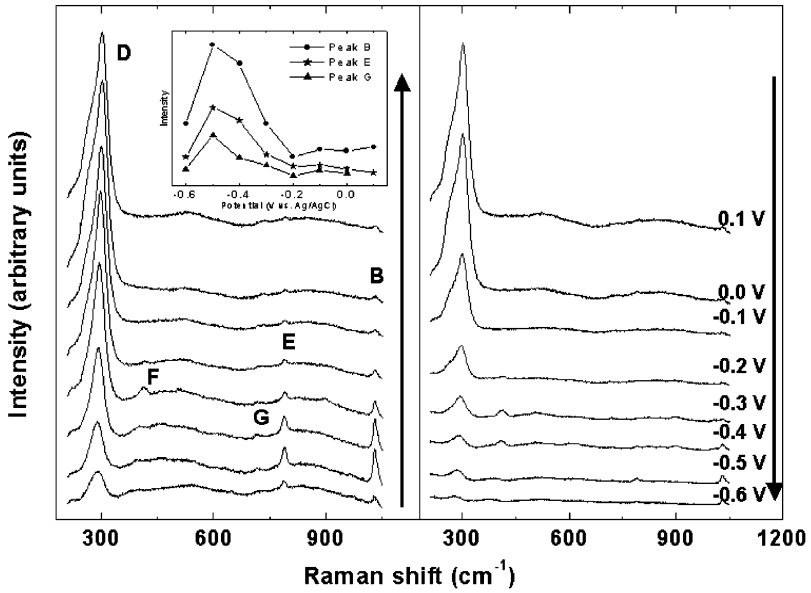

Figure 3. Surface-enhanced Raman spectra (250−1100 cm^{-1} region) of Cu(poly) in 2 mM KCl + 10 mM $CuSO_4$ + 0.1 M H_2SO_4 at various potentials during anodic steps (left panel) and cathodic steps (right panel). Insert: SERS peak intensity as a function of potential during anodic steps for peaks B, E, and G.

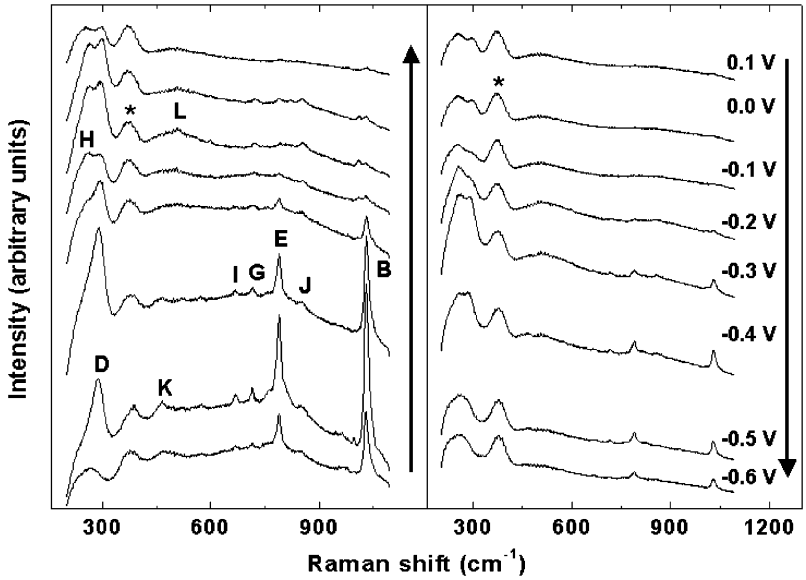

Figure 4. Surface-enhanced Raman spectra (250−1100 cm^{-1} region) of Cu(poly) in 88 μM poly(ethylene glycol) + 2 mM KCl +10 mM $CuSO_4$ + 0.1 M H_2SO_4 at various potentials during anodic steps (left panel) and cathodic steps (right panel).

In a second control experiment directed at establishing the identities of peaks E and G, we examined the SERS from Cu in a solution containing 0.1 M H_2SO_4 + 2 mM KCl, but without any added $CuSO_4$. In these measurements, peaks E and G were not observed. This behavior indicates that peaks E and G are most likely related to the presence of Cu^{2+}. An additional requirement for peaks E and G seems to be K^+, since these peaks are only apparent when KCl or KBr is added to the electrolyte, but are independent of halide identity. Calculations examining the interaction of HSO_4^- with chelating cations indicate that two of the four Raman and IR active S−O stretching bands are cation dependent.[38] Among these is the S−O(H) stretching band, which lies in the range of 700−880 cm^{-1} depending on the cation type. The Raman frequencies for this stretch have been reported to be at 873 cm^{-1} for solid $KHSO_4$[38] and 869 cm^{-1} in supersaturated aqueous $KHSO_4$.[39] The possible enhancement of bisulfate adsorption by the presence of Cu^{2+} has been discussed above. Although such a cation-chelated bisulfate species is not abundant enough in bulk solution to generate an observable band in the solution spectrum (Figure 2b), its localization on the surface may lead to a signal in the SERS. In sum, peaks E and G are associated with stretching modes in a K^+ chelated bisulfate species that are enhanced by the presence of Cu^{2+}.

3.2.1.3. With Both PEG and Cl$^-$. Figure 4 shows SERS obtained from a Cu surface in solution containing 2 mM Cl^- and 88 μM PEG in addition to the 0.1 M H_2SO_4 and 10 mM $CuSO_4$ used previously. In addition to peaks B, D, E, and G, which were observed in solutions containing Cl^- without PEG, the spectrum reveals additional potential-dependent features at 260 cm^{-1} (peak H), 669 cm^{-1} (peak I), 850 cm^{-1} (peak J), 460 cm^{-1} (peak K), and 520 cm^{-1} (peak L). These new features provide considerable information about the synergy between Cl^-, PEG, aqueous Cu, and the Cu surface.

Peak H starts to grow as a shoulder on the Cu(surface)−Cl stretch band (peak D) at −0.3 V during the anodic scan and

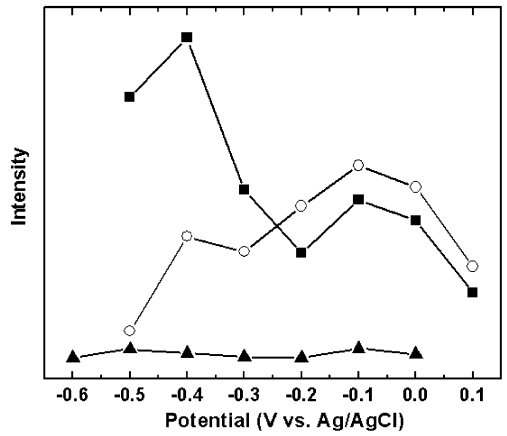

Figure 5. SERS peak intensity as a function of potential for Cu in 88 μM poly(ethylene glycol) + 2 mM KCl +10 mM $CuSO_4$ + 0.1 M H_2SO_4 during anodic steps for the 290 cm^{-1} band (peak D) (square), the 260 cm^{-1} band (peak H) (open circle), and the 850 cm^{-1} band (peak J) (triangle).

grows relative to this band as the potential is swept to more positive values. Figure 5 depicts the intensity dependence of peak D, H, and J upon potential variation when the potential is moved in the anodic direction. The potential dependence of the intensity of peak D is unlike that found in Figure 3, which was obtained without PEG. In Figure 3, the intensity of peak D increases linearly as the potential is swept to more positive values. Along with this intensity increase is a shift in frequency, from 289 to 302 cm^{-1}, consistent with the Stark shift expected.[27,37] In the presence of PEG, peak D is most intense at −0.4 V. The intensity then decreases significantly as the potential moves to further positive values. The Stark shift is difficult to observe when PEG is added, because of the overlap of peaks D and H. Peak H increases in intensity on the anodic potential sweep from −0.5 to −0.1 V, and maximizes at −0.1 V. At further positive potentials, the intensity of both peak D and H decrease moderately, which may be due to the anodic dissolution of Cu at these positive potentials.

The energy of peak H suggests that it—like peak D—is associated with a Cu−Cl stretch. However, the 30 cm^{-1} red-shift of peak H relative to peak D indicates that the Cu−Cl bond is weaker in the species associated with peak H. One possible reason for this reduction in frequency is that the Cu species is no longer metallic, but rather part of a complex. We show below that calculations strongly support assignment of peak H (and peaks K, L, and I in this figure) as arising from a Cl−Cu−PEG complex. Furthermore, when chloride ion is substituted with bromide again in this solution, the frequencies for bands at lower wavelength are very different from those observed here in the chloride-containing solutions (spectra not shown). The disappearance of both peaks H and D upon halide substitution supports the assignments of Cu−Cl stretches to band D and H.

Peak J at 850 cm^{-1} is associated with PEG because its position is identical to that found in the normal Raman spectrum of PEG in water (Figure 1b). The 850 cm^{-1} band was found to be the strongest in the normal Raman spectrum of PEG. The presence of this band in the SERS spectrum is strong evidence that PEG is adsorbed on or near the Cu electrode surface. Figure 5 shows that the potential dependence of peak J (triangles) is not nearly as significant as that of peaks D (square) and H (circle), which suggests that the amount of PEG on the surface is independent of potential.

There are three other bands seen in Figure 4 which are associated with the presence of PEG, Cl^-, and Cu in the electrolyte. Peak K at 465 cm^{-1} appears at potentials negative of −0.3 V. At potentials more positive than −0.3 V, this peak is replaced by a new band at higher frequency, 510 cm^{-1} (peak L). Both these peaks are broader than others seen in these spectra. These bands appear in a spectral region that has been associated with Cu−O vibrational modes.[31,40] However, these Cu−O features are typically observed in neutral or basic electrolyte, not in acidic media used here. The calculation described below will establish that both of these bands are likely associated with Cu−O vibrational modes in a Cl−Cu−PEG complex. Finally, peak I at 670 cm^{-1} peaks in intensity at −0.5 V. This band is also assigned to an internal mode of the Cl−Cu−PEG complex.

3.2.2 Au Electrode Surface. Figure 6 shows SERS obtained from a roughened Au surface in a solution containing 0.1 M H_2SO_4 + 2 mM KCl + 88 μM PEG. $CuSO_4$ was not added to the solution in order to prevent Cu from depositing onto the Au surface. The spectra shown here have been flattened using background subtraction.

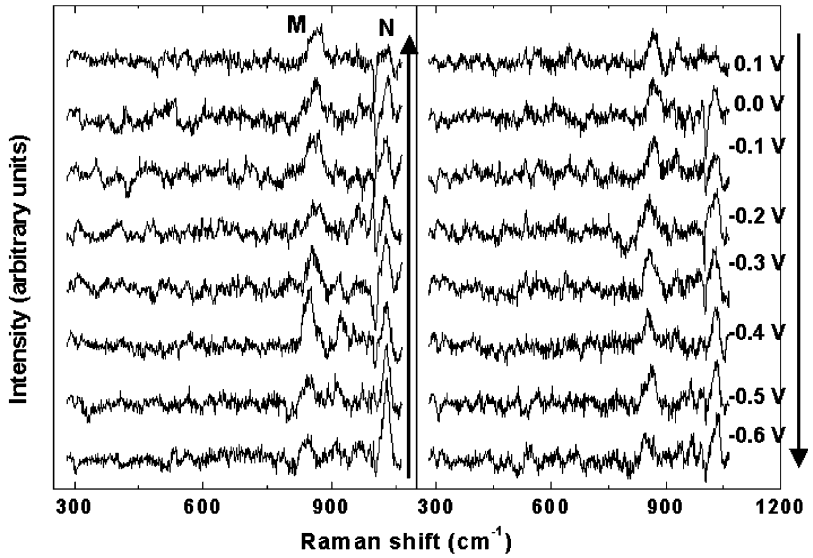

Figure 6. Surface-enhanced Raman spectra (280−1100 cm^{-1} region) of Au(poly) in 88 μM poly(ethylene glycol) + 2 mM KCl + 0.1 M H_2SO_4 at various potentials during anodic steps (left panel) and cathodic steps (right panel).

The spectra show a number of differences relative to those obtained from a Cu surface. First, no peaks are observed in the region below 300 cm^{-1}. The Au−Cl stretch should occur between 250 and 260 cm^{-1},[41,42] and the lack of a feature in the spectrum indicates that Cl is not present on the surface at the potentials used here. Weaver and co-workers found that Cl formed an overlayer on Au only at potentials more positive than those relevant for Cu deposition.[43] Second, a band is observed around 850 cm^{-1} in these spectra throughout the potential range studied (peak M). The intensity of this band is independent of potential. Measurements made from solutions containing Cl^- but not PEG did not show this band, which suggests that it is PEG-related. The band is likely associated with the C−O stretch in the PEG unit, similar to peak J observed on the Cu surface.

Several other peaks are observed at frequencies between 900 and 1050 cm^{-1}. The major one at 1030 cm^{-1} (peak N) shows potential dependence. This peak is assigned to the symmetric stretch of the S−O band in bisulfate on Au.[44] The intensity of this peak decreases as the potential moves to more positive values. This behavior is similar to that of peak B observed at this frequency on the Cu surface, which is associated with the symmetric stretch of S−O bond in bisulfate on Cu.

3.3. Calculations. To clarify the origins of peaks H, I, K, and L and associate these with particular PEG−Cu−Cl complexes, we performed calculations on two model compounds using the Spartan software package. Studies of overpotential with solution composition emphasize a role for PEG, Cl^-, and Cu in describing the PEG interaction with the Cu surface.[5,7,9,35] Known Cu(I) complexes exhibit linear (2 ligands), trigonal (3 ligands), or tetrahedral (4 ligands) coordination geometries.[45] Previous work examining the dependence of over-potential with extent of polymerization showed that 7 to 10 monomer PEG units is to be the minimal possible composition for PEG to influence the over-potential.[8] Conformational studies on PEG in aqueous solutions suggest that PEG stays in a helical structure with 7 monomers per repeating unit.[23,24,46,47] Initial models of PEG coordination to Cu featured a seven-coordinate Cu center.[8] However, paramagnetic resonance measurements examining Cu^{2+} coordination with PEG concluded that Cu was associated with only one ether oxygen from PEG with the balance from water,[13] a view that was echoed by Stoychev and Tsvetanov.[10] Seven-coordinate Cu complexes are rare.

Figure 7 shows our models for the PEG−Cu−Cl complex. Hydrogen atoms are not shown for clarity. Here, we utilize a Cu(I) center which is complexed by two O from PEG and one Cl^- ligand. Higher coordination numbers are not typically found in aqueous Cu(I) chemistry, and the presence of a Cu−Cl bond is clear from the spectroscopy. This limits the degree of interaction between PEG and Cu. To facilitate the calculation, the PEG part of the molecule was limited to three or four PEG monomer units.

In both models, copper has a three-coordinated structure, with two oxygen ligands and one chloride ligand. Table 3 lists the optimized bond lengths and bond angles for these models. The major difference between the two models is the position at which the Cu atom associates with the polymer chain. Because the PEG has both termini ending with CH_2−OH, there are only two possible types of oxygen atoms the Cu could bind with: an ether O in the CH_2−O−CH_2 chain, and an hydroxyl O at the CH_2−O−H end. Model I has Cu binding with two identical oxygen atoms in the middle of the polymer chain, while model II involves one of the terminal oxygen atoms.

Table 3 shows that there are only small differences in the bond lengths between the two models. In particular, both Cu−Cl bond lengths and both Cu−O(2) bond lengths are nearly identical. The Cu−Cl bond length is calculated to be 2.12 Å for both models, and that of the Cu−O(2) are 1.83 and 1.81 Å for models I and II, respectively. The Cu−O(1) bond length is slightly different due to the different groups that are attached to the O(1) atom. They are 2.15 Å in model I and 2.21 Å in model II. All C−O and C−C bond lengths in the energy-minimized models are similar to that found for the free, helically structured PEG molecule in the aqueous environment. Specifically, the C−O bond length is calculated to be an average of 1.44 Å, compared with 1.40 Å found experimentally, while the C−C bond is calculated to be 1.52 Å long on average, compared with 1.51 Å found experimentally.[23]

We next consider higher coordination numbers for the Cu center. Given that the PEG moiety remains helical in solution, and given the relatively normal Cu−O bond lengths inferred from the spectroscopy, we consider the Cu−O bond length required for a four-coordinate Cu(I) center. Without distorting the PEG helix, subsequent Cu−O bond lengths are calculated to be on the order of 5.5 Å. This distance is outside of that normally found for Cu−O complexes, which is normally in the

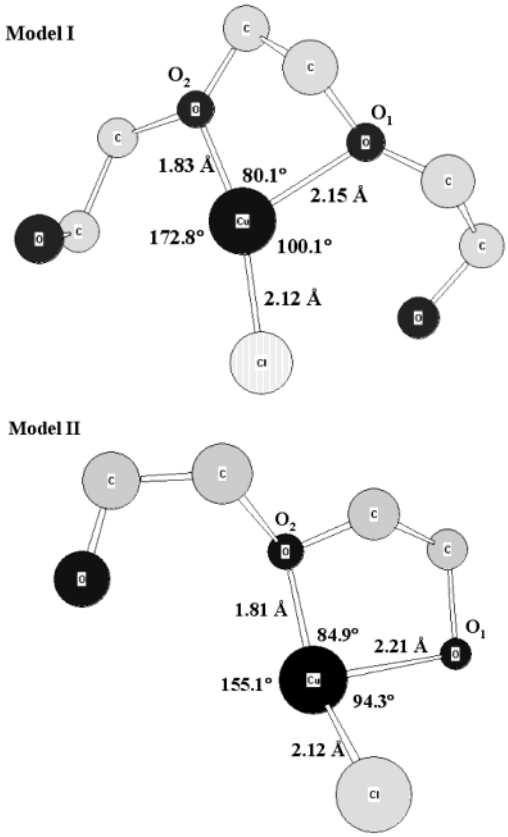

Figure 7. Structural models of two PEG−Cu−Cl complexes; Model I: Cu atom is associated with two ether oxygen atoms of PEG and one chloride ligand; Model II: Cu atom is associated with one ether oxygen atom and one hydroxyl oxygen atom of PEG and one chloride ligand.

TABLE 3: Bond Lengths and Bond Angles of the Proposed Models

geometry	Model I	Model II
d(Cu−Cl) (Å)	2.12	2.12
d(Cu−O_1) (Å)	2.15	2.21
d(Cu−O_2) (Å)	1.83	1.81
∠(Cl−Cu−O_1) (°)	100.1	94.3
∠(Cl−Cu−O_2) (°)	172.8	155.1
∠(O_1−Cu−O_2) (°)	80.1	84.9

TABLE 4: Calculated Vibrational Frequencies and Band Assignments for PEG−Cu−Cl Complex

	frequencies (cm^{-1})			
mode	Model I	Model II	assignment	corresponding peak
1	230	205	δCu−Cl	
2	267	265	ν Cu−Cl	H (260 cm^{-1})
3	290	298		
4	292	302	δ Cu−O	
5	305			
6	460	396	ν Cu−O	K (465 cm^{-1})
7	483	485		
8	504	562	ν_{as} Cu−O	L (510 cm^{-1})
9	548			
10	696	838	δ O−C−C−O	I (670 cm^{-1})

vicinity of 2 Å.[48−50] A distorted PEG could accommodate higher coordination numbers around the Cu center, but there is no evidence for this distortion in the spectroscopy. Hence, coordination numbers higher than three around the Cu center are unlikely.

The differences in bond angles between the two models are more significant. In model I, the bond angles around the Cu atom are: 80.1° for O(2)−Cu−O(1), 100.1° for O(1)−Cu−Cl, and 172.8° for O(2)−Cu−Cl. The corresponding angles in model II are 84.9°, 94.3°, and 155.1°, respectively. The three-coordinate Cu complexes are nearly planar in both models. Both Cl−Cu−O angles in model II are smaller than those of model I. This behavior could be due to the smaller hindrance of the OH group comparing with that of the $O-CH_2-CH_2-O$ group.

Table 4 lists the calculated frequencies and their assignments for both models in the frequency region from 200 to 800 cm^{-1}. There are fewer modes associated with model II because this model features fewer atoms. The energies associated with most of the vibrational modes of the Cu−O and Cu−Cl bonds lie in this region. The frequencies associated with the Cu−Cl stretch are calculated at 267 and 265 cm^{-1} for models I and II, respectively. These results agree well with the experimental observation of 260 cm^{-1}. Bands associated with Cu−O stretching modes are calculated to lie between 396 cm^{-1} and 562 cm^{-1} (modes 6 to 9). Experimentally, this range is in agreement with energies reported for Cu(I)−O stretches in species such as Cu_2O.[31,40] The calculation indicates that the symmetric stretch of the Cu−O bond lies in the range between 396 and 485 cm^{-1}. Peak K at 465 cm^{-1} falls right in this range. The asymmetric stretch of the Cu−O bond is calculated to lie in the region from 504 to 562 cm^{-1}. This region includes peak L at 510 cm^{-1}, which is therefore assigned to this mode. At higher frequencies, the calculation indicates that the modes are mainly associated with internal vibration of the PEG part of the molecule. In Model I, a mode is found at 696 cm^{-1}, which is associated with a bending vibration of the O−C−C−O part of the PEG molecule between the Cu-linked oxygen atoms. This energy is close to that observed for peak I at 670 cm^{-1}. Model II does not generate a mode in this region of the spectrum, but does find a similarly assigned vibration at 838 cm^{-1}. Overall, the Cu−O vibrations predicted by model I match better with what we have observed experimentally. This observation may suggest that model I is a more likely species to account for the PEG−Cu−Cl association.

The calculation reveals other modes associated with Cu−Cl bending and Cu−O bending modes that are apparently not observed in the SER spectrum. The Cu−Cl bending modes may be too low in energy to be seen in our measurements, while the Cu−O bending modes apparently overlap with the intense Cu_{surf}−Cl stretch (peak D at 290 cm^{-1}).

4. Discussion

4.1. Coordination Environment for the Cl−Cu−PEG Complex. The measurements performed here provide strong evidence for the existence of the Cl−Cu−PEG complex at the Cu electrode surface. The presence of a lower energy band at 260 cm^{-1} which occurs only on addition of all of solution Cu, Cl^-, and PEG strongly suggests that Cu is associated with Cl in the complex. In addition, the occurrence of a band associated with the PEG molecule by itself (peak J), which also is present in the spectroscopy only when all of the solution constituents are in place, suggests that part of this complex involves the PEG molecule.

Calculations and detailed assignments of what is a fairly complex system support the idea of Cu−O coordination to PEG. We found that the spectroscopy could be reasonably explained by a model involving coordination of Cu to two O of the PEG molecule in addition to the one Cl. Again, the presence of the Cu−O bands only when all three solution constituents are present strongly supports the notion of Cu−PEG coordination.

4.2. Potential Dependence. The potential dependence of the peaks that are associated with the Cl−Cu−PEG complex gives insights to the adsorption−desorption process with changing potentials. The peaks of interest are peak H, K, L, I, and J, which are PEG complex structure-related.

Peak H is associated with the bridging Cu−Cl stretch in the complex. The intensity of this peak increases as the potential moves to more positive values from −0.5 V to −0.1 V. This behavior suggests that this complex starts to adsorb on the Cu surface at −0.5 V, and the interaction between the complex and the Cu surface remains strong even at the Cu open circuit potential (−0.15 V vs Ag/AgCl). This behavior is in good agreement with previous electrochemical and spectroscopic studies.[8−10] Healy et al.[7] also concluded that a PEG species was formed at open circuit potential. The decrease in intensity of peak H at more negative potential is expected because chloride adsorption becomes weaker upon cathodic potential excursion and eventually desorbs from the surface. This leads to desorption of the complex.

Peaks K and L are both associated with the symmetric and asymmetric Cu−O stretching mode in the complex, respectively. Peak L shows a potential dependence similar to that of peak H. Alternatively, peak K is found at negative potentials, but disappears by −0.3 V. Peak I exhibits the same behavior. One possible explanation for this behavior is reorientation of the PEG complex as a function of applied potential, wherein the degree of Cl−Cu−PEG coordination becomes progressively less at more negative potentials. However a detailed understanding of this behavior would require a more detailed assignment of the spectroscopy.

The potential dependence of peak J is relatively more straightforward. Since this peak is a direct indication for adsorption of PEG molecules, it can also provide information on the potential-dependent adsorption of the polymer on the surface. Peak H shows a clear potential dependence indicating that the complex is desorbed at more negative potentials. It is interesting that at more negative potential, peak J remains even though peak H has disappeared. Healy et al. proposed that PEG adsorbs on the Cu surface in the presence of chloride in two forms, complexed with Cu at near open circuit potential, and neutral at more negative potentials.[7] It is possible that the PEG-related peaks seen at more negative potentials are due to the physisorption of the molecule.

4.3. Significance of Cu Surface. On Au the presence of a peak at 850 cm^{-1} suggests that PEG molecules are associated

with the Au surface. The absence of peaks involving coordination to Au, which would be expected in the region below ca. 600 cm^{-1}, suggests that PEG associated to the Au surface is weak. It is important to note that while PEG adsorption to Cu leads to a rich spectroscopy, indicating a significant role for all of Cu, Cl, and PEG, this kind of interaction is not observed on the Au surface. This suggests a significant role for Cu in PEG association. The possibility of PEG adsorption on Au surfaces has been shown in a QCM study,[2] where modest, potential-insensitive interaction was inferred.

4.4. Mechanism of Inhibition. PEG molecules are believed to inhibit Cu deposition by forming a physical barrier to prevent Cu^{2+} or Cu^{+} from diffusing to the Cu surface in an electroplating bath. Yet a large amount of electrochemical and nonelectrochemical work have shown that PEG does not adsorb on bare Cu surface easily. Complex formation among PEG, cuprous ion, and chloride ions in Cu electroplating solution, initially proposed by Yokoi et al., has been a widely accepted explanation for the observation that PEG adsorbs strongly on the Cu surface only in the presence of chloride ions.[8] By systematically adding PEG and chloride to the Cu electroplating bath, the SERS spectra provide significant information on the synergic effect of PEG, Cu, and chloride.

On the basis of the SERS spectra and the computer modeling discussed above, we propose a three-coordination Cu with two ether oxygen ligands from PEG and one chloride ligand. In our models, we consider both the Cu-linked oxygen atom from either an ether oxygen in the PEG chain (model I), or a hydroxyl oxygen at the end of PEG chain (model II). Comparing the frequencies observed in SERS experiments with those calculated, it suggests that model I provides a better match than model II. This observation could be rationalized considering the higher probability of Cu linking to an ether oxygen rather than a much less abundant hydroxyl oxygen.

The requirement for inhibition, based on these models are as follows: (a) the molecule forms a strong bond with the electrode surface, in this case through a bridging Cl^{-}; (b) the molecule features a protected Cu(I) center with restricted access of this center to the electrolyte; (c) the molecule features a critical organic content without which there is little inhibition. In this case, previous work has shown that the full inhibitory action of PEG does not develop until sufficient PEG subunits are available to form one full repeating unit of the PEG polymer helix.[8] The helix apparently prevents approach of electrolyte to the metal center.

It is interesting to note that the overpotential developed by the PEG/Cl/Cu system (ca. 380 mV vs Cu^{2+}/Cu) is not dissimilar from that developed by another inhibitor, benzotriazole (BTA) (ca. 410 mV vs Cu^{2+}/Cu) under similar conditions.[51] The inhibiting action of BTA originates in the formation of a polymeric complex with Cu(I), wherein each BTA is coordinated to two Cu(I) centers.[52,53] The polymer prevents association of electrolyte with the Cu surface.

5. Conclusions

The SER spectroscopic results presented here confirm the significant enhancement by chloride ion to the adsorption of PEG in acidic Cu electroplating bath. Additional bands observed in the SER spectra with the presence of both PEG and chloride indicate the formation of a PEG−Cu−Cl species at the surface. On the basis of the spectroscopic data, two models of a three-coordinated Cu center associated with two oxygen atoms from PEG and one chloride ligand are constructed. Ab initio calculations of the vibrational modes of the models facilitate the assignments of the peaks observed. SERS experiments carried out on Au surface with PEG and chloride in the absence of Cu^{2+} do not generate complex-related peaks, which indicates the importance of Cu species in the complex formation.

Acknowledgment. This work was funded by Department of Energy Grant DE-FG02-91ER45349 through the Materials Research Laboratory at the University of Illinois. Z.V.F. acknowledges a departmental fellowship in Chemistry. X.L. thanks the Department of Chemistry for financial support in the form of a Carl Shipp Marvel fellowship. The authors thank R. Strange and J. O. White of the Laser Laboratory in the Frederick Seitz Materials Research Laboratory at the University of Illinois for their assistance in Raman data acquisition. The Laser Laboratory is funded by Department of Energy Grant DE-FG02-96ER45439 through the Materials Research Laboratory at the University of Illinois.

References and Notes

(1) Andricacos, P. C.; Uzoh, C.; Dukovic, J. O.; Horkans, J.; Deligianni, H. *IBM J. Res. Dev.* **1998**, *42*, 567−574.
(2) Kelly, J. J.; West, A. C. *J. Electrochem. Soc.* **1998**, *145*, 3472−3476.
(3) Stafford, G.; Moffat, T.; Javic, V.; Kelley, D.; Bonevich, J.; Josell, D.; Vaudin, M.; Armstrong, N.; Huber, W.; Stainshevsky, A. *Cu electrodeposition for on-chip interconnections*, 1st ed.; Seiler, D. G., Diebold, A. C., Shaffner, T. J., McDonald, R., Bullis, W. M., Smith, P. J., Secular, E. M., Eds.; Springer-Verlag: Berlin, 2000; pp 402−406.
(4) Dini, J. W. *Electrodeposition of Cu*, 4th ed.; Schlesinger, M., Paunovic, M., Eds.; John Wiley & Sons: New York, 2000; pp 61−119.
(5) Reid, J. D.; David, A. P. *Plat. Surf. Finish.* **1987**, *74*, 66−70.
(6) Pearson, T.; Dennis, J. K. *J. Appl. Electrochem.* **1990**, *20*, 196−208.
(7) Healy, J. P.; Pletcher, D. *J. Electroanal. Chem.* **1992**, *338*, 155−165.
(8) Yokoi, M.; Konishi, S.; Hayashi, T. *Denki Kagaku* **1984**, *52*, 218−223.
(9) Hope, G. A.; Brown, G. M. *Electrochem. Soc. Prec.* **1996**, *96*−*8*, 215−226.
(10) Stoychev, D.; Tsvetanov, C. *J. Appl. Electrochem.* **1996**, *26*, 741−749.
(11) Kang, M.; Gewirth, A. *J. Electrochem. Soc.* **2003**, *150*, C426−C434.
(12) Hayase, M.; Taketani, M.; Azawa, K.; Hatsuzawa, T.; Hayabusa, K. *Electrochem. Solid-State Lett.* **2002**, *5*, C98−C101.
(13) Suryanarayana, D.; Narayana, P. A.; Kevan, L. *Inorg. Chem.* **1983**, *22*, 474−478.
(14) Weaver, M. J. *J. Raman Spectrosc.* **2002**, *33*, 309−317.
(15) Campion, A.; Kambhampati, P. *Chem. Soc. Rev.* **1998**, *27*, 241−250.
(16) Garrell, R. L. *Anal. Chem.* **1989**, *61*, 401A−411A.
(17) Biggin, M. E. In situ vibrational spectroscopic and electrochemical study of electrodeposition additives on Cu surfaces. Ph.D. Thesis, University of Illinois-Urbana, 2001, p 147.
(18) Matsuura, H.; Fukuhara, K. *J. Mol. Struct.* **1985**, *126*, 251−260.
(19) Matsuura, H.; Fukuhara, K.; Takashima, K. *J. Phys. Chem.* **1991**, *95*, 10800−10810.
(20) Fukushima, K.; Matsuura, H. *J. Mol. Struct.* **1995**, *350*, 215−219.
(21) Harranen, J.; Kinnunen, J.; Mattsson, B.; Rine, H.; Sundholm, F.; Torell, L. *Solid State Ionics* **1995**, *80*, 201−212.
(22) Matsuura, H.; Fukuhara, K.; Masatoki, S.; Sakakibara, M. *J. Am. Chem. Soc.* **1991**, *113*, 1193−1202.
(23) Tadokoro, H.; Chatani, Y.; Yoshihara, T.; Tahahra, S.; Murahashi, S. *Makromol. Chem.* **1964**, *73*, 109−127.
(24) Begum, R.; Matsuura, H. *J. Chem. Soc., Faraday Trans.* **1997**, *93*, 3839−3848.
(25) Yang, X.; Su, Z.; Wu, D.; Hsu, S. L.; Stidham, H. D. *Macromolecules* **1997**, *30*, 3796−3802.
(26) Brown, G. M.; Hope, G. A. *J. Electroanal. Chem.* **1995**, *382*, 179−182.
(27) Niaura, G.; Malinauskas, A. *J. Chem. Soc., Faraday Trans.* **1998**, *15*, 2205−2211.
(28) Gillespie, R. J.; Robinson, E. A. *Can. J. Chem.* **1962**, *40*, 644−657.
(29) Brown, G. M.; Hope, G. A. *J. Electroanal. Chem.* **1996**, *413*, 153−160.

(30) Brown, G. M.; Hope, G. A. *J. Electroanal. Chem.* **1996**, *405*, 211−216.
(31) Chan, H. Y. H.; Takoudis, C. G.; Weaver, M. J. *J. Phys. Chem. B* **1999**, *103*, 357−365.
(32) LaGraff, J. R.; Gewirth, A. A. *Surf. Sci.* **1995**, *326*, L461.
(33) Cruickshank, B. J.; Sneddon, D. D.; Gewirth, A. A. *Surf. Sci.* **1993**, *281*, L308.
(34) Kelly, J. J.; Tian, C.; West, A. C. *J. Electrochem. Soc.* **1999**, *146*, 2540−2545.
(35) Bonou, L.; Eyraud, M.; Denoyel, R.; Massiani, Y. *Electrochim. Acta* **2002**, *47*, 4139−4148.
(36) Stoychev, D. S.; Vitanova, I.; Rashkov, S.; Vitanov, T. *Surf. Technol.* **1978**, *7*, 427−432.
(37) Niaura, G.; Malinauskas, A. *Chem. Phys. Lett.* **1993**, *207*, 455−460.
(38) Sawatari, Y.; Sueoka, T.; Shingaya, Y.; Ito, M. *Spectrochim. Acta* **1994**, *50A*, 1555−1561.
(39) Fung, K. H.; Tang, I. N. *Chem. Phys. Lett.* **1989**, *163*, 560−564.
(40) Niaura, G. *Electrochim. Acta* **2000**, *45*, 3507−3519.
(41) Holze, R. *Surf. Sci.* **1988**, *202*, L612−L620.
(42) Gao, P.; Patterson, M. L.; Tadayyoni, M. A.; Weaver, M. J. *Langmuir* **1985**, *1*, 173−176.
(43) Gao, P.; Weaver, M. J. *J. Phys. Chem.* **1986**, *90*, 4057−4063.
(44) Socrates, G. *Inorganic compounds and coordination complexes*; Wiley: Chichester, New York, 2001.
(45) Wells, A. F. *Structural Inorganic Chemistry*, 5th ed.; Clarendon Press: Oxford, 1984.
(46) Oesterhelt, F.; Rief, M.; Gaub, H. E. *New J. Phys.* **1999**, *1*, 6.1−6.11.
(47) Yang, R.; Yang, X. R.; Evans, D. F.; Hendrickson, W. A.; Baker, J. *J. Phys. Chem.* **1990**, *94*, 6123−6125.
(48) Darensbourg, D. J.; Holtcamp, M. W.; Reibenspies, J. H. *Polyhedron* **1996**, *15*, 2341−2349.
(49) Ozutsumi, K.; Kawashima, T. *Polyhedron* **1992**, *11*, 169−175.
(50) Feiters, M. C.; Gebbink, R. J. M. K.; Sole, V. A.; Nolting, H.-F.; Karlin, K. d.; Nolte, R. J. M. *Inorg. Chem.* **1999**, *38*, 6171−6180.
(51) Kang, M.; Gross, M. E.; Gewirth, A. A. *J. Electrochem. Soc.* **2003**, *150*, C292−301.
(52) Magnussen, O. M.; Vogt, M. R.; Scherer, J.; Behm, R. J. *Appl. Phys. Mater. Sci. Proc.* **1998**, *A66*, S447−S451.
(53) Vogt, M. R.; Nichols, R. J.; Magnussen, O. M.; Behm, R. J. *J. Phys. Chem. B* **1998**, *102*, 5859.